Food web framework for size-structured populations

Martin Hartvig, Ken H. Andersen, Jan E. Beyer

Food web framework for size-structured populations

Martin Hartvig, Ken H. Andersen, Jan E. Beyer

PII: S0022-5193(10)00661-2
DOI: doi:10.1016/j.jtbi.2010.12.006
Reference: YJTBI6275

To appear in: *Journal of Theoretical Biology*

Received date: 22 September 2010
Revised date: 2 December 2010
Accepted date: 4 December 2010

Cite this article as: Martin Hartvig, Ken H. Andersen and Jan E. Beyer, Food web framework for size-structured populations, *Journal of Theoretical Biology*, doi:10.1016/j.jtbi.2010.12.006

Food web framework for size-structured populations

Martin Hartvig[a,*], Ken H. Andersen[b], Jan E. Beyer[b]

[a] *Department of Theoretical Ecology, Lund University, Ecology Building, SE-223 62 Lund, Sweden*
[b] *DTU Aqua, National Institute of Aquatic Resources, Technical University of Denmark (DTU), Charlottenlund Slot, Jægersborg Allé 1, DK-2920 Charlottenlund, Denmark*

Abstract

We synthesise traditional unstructured food webs, allometric body size scaling, trait-based modelling, and physiologically structured modelling to provide a novel and ecologically relevant tool for size-structured food webs. The framework allows food web models to include ontogenetic growth and life-history omnivory at the individual level by resolving the population structure of each species as a size-spectrum. Each species is characterised by the trait 'size at maturation', and all model parameters are made species independent through scaling with individual body size and size at maturation. Parameter values are determined from cross-species analysis of fish communities as life-history omnivory is widespread in aquatic systems, but may be reparameterised for other systems. An ensemble of food webs is generated and the resulting communities are analysed at four levels of organisation: community level, species level, trait level, and individual level. The model may be solved analytically by assuming that the community spectrum follows a power law. The analytical solution provides a baseline expectation of the results of complex food web simulations, and agrees well with the predictions of the full model on 1) biomass distribution as a function of individual size, 2) biomass distribution as a function of size at maturation, and 3) relation between predator-prey mass ratio of preferred and eaten food. The full model additionally predicts the diversity distribution as a function of size at maturation.

Keywords: community ecology, trait based model, life-history omnivory, ontogeny, size-spectrum

1. Introduction

Food webs are typically modelled using unstructured species populations based on generalised Lotka-Volterra equations. This unstructured formulation ignores individual life-history by assigning a fixed trophic position to all individuals within a species. In aquatic ecosystems this assumption is violated as fish offspring reside at a low trophic level and grow during ontogeny through multiple trophic levels before reaching maturation (Werner and Gilliam, 1984). Along this journey, from the milligram range and up to several kilogram, fish change diet (as well as enemies) and consequently exhibit life-history omnivory through preying on different trophic levels in different life-stages (Pimm and Rice, 1987). Thus the assignment of a unique trophic level and role (resource, consumer, predator, etc.) for species in unstructured models is incompatible with systems where ontogenetic growth and life-history omnivory are pronounced. In the cases where

*Corresponding author.
Email addresses: Martin.Pedersen@teorekol.lu.se / martin@hvig.dk (Martin Hartvig), kha@aqua.dtu.dk (Ken H. Andersen), jeb@aqua.dtu.dk (Jan E. Beyer)

trophic level of individuals within a species is positively correlated with body size (Jennings et al., 2002), individual size may be used as a proxy for trophic level. Models may therefore account for ontogenetic growth and life-history omnivory by resolving the size-structure within each species.

A general framework for large food webs that includes the size-structure for all species must fulfil a set of requirements. It should: 1) be generic in the sense that large species-specific parameter sets are not necessary, 2) be based on mechanistic physiological individual-level processes, where parameters represent measurable biological quantities, 3) resolve food dependent growth of individuals (Werner and Gilliam, 1984), 4) be practically solvable for species-rich systems over many generations, and 5) comply with empirical data on size-structured communities. In this work we develop a food web framework complying with these requirements by resolving the life-history of individuals within species by a continuous size-spectrum. We parameterise the model for aquatic systems as an example of a size-structured community with widespread life-history omnivory, but the framework may be parameterised for other system types (cf. Discussion). In fish communities the most prominent empirical patterns, which the model framework should comply with, are that individuals exhibit biphasic growth (Lester et al., 2004), and the Sheldon community spectrum. Sheldon et al. (1972) hypothesised that the community biomass spectrum, from bacteria to whales, as a function of body mass is close to constant. Empiric studies later showed that the biomass for fish indeed is close to constant or slightly declining as a function of body mass (Ursin, 1982; Boudreau and Dickie, 1992) with the complication that heavily fished systems have a steeper decline in biomass (Jennings et al., 2002; Daan et al., 2005).

The importance of resolving ontogenetic growth and life-history omnivory has long been realised in fisheries science, where mechanistic individual-level size-structured food web models of fish communities were pioneered (Andersen and Ursin, 1977). Independently, the physiologically structured population model (PSPM) framework (Metz and Diekmann, 1986; de Roos and Persson, 2001) has been developed in the field of ecology. While providing the ecological realism needed for a size-structured food web framework these approaches typically rely on large species-dependent parameter sets, which must be reduced for the approaches to be useful as generic frameworks.

Reduction to species-independent parameter sets has been achieved in unstructured models of interacting populations by scaling of physiological and demographic rates with body size (Yodzis and Innes, 1992). By using body size as a trait this approach has resulted in several simple generic food web models for unstructured populations (Loeuille and Loreau, 2005; Virgo et al., 2006; Brose et al., 2006b; Lewis and Law, 2007).

In this work we combine the two approaches into one unified framework: We 1) use a physiological based description of individual life-history, and 2) use a single trait (size at maturation) to characterise each species while using trait and body size scaling to get one condensed species-independent parameter set. All processes are based on descriptions at the level of individuals, and interaction strengths among individuals are dynamic through the prescription of size-dependent food selection. This leads to a realised effective food web structure which depends on the emergent

size-spectrum composition of all species. In this manner we synthesise a general framework that in a conceptually simple yet ecologically realistic way can be used to model food webs where the life cycle of individuals in each species is explicitly modelled from birth to reproduction and death.

Our primary objective is the formulation and parametrisation of the food web framework. Food webs generated by unstructured food web models may be analysed at the community level in terms of distributions of biomass across species and trophic levels. Trait-based size-structured food webs allow a more detailed analysis of the community level as well as enabling analysis on three additional levels of organisation: 1) at the community level, i.e., the distribution of total biomass as a function of body size of individuals regardless of their species identity, and the distribution of biomass and diversity as a function of the trait size at maturation, 2) at the species level, i.e., distribution of biomass as a function of size within a given species, 3) at the trait level, which in the case of a single trait equals the species level, and 4) at the individual level, i.e., distribution of size of food in the stomachs. Due to this added complexity of size-structured food webs, our secondary objective is to illustrate diversity and biomass distributions at different levels of organisation. To this end we generate an ensemble of food webs and analyse them in terms of distributions of average community size-spectra, species size-spectra, trait biomass distributions, and trait diversity distributions. Finally, we develop an analytical solution of the model framework, basically by assuming that the community spectrum follows a power-law (equilibrium size-spectrum theory, EQT). All distributions, except the diversity distribution, may be calculated from EQT, and we demonstrate general accordance between EQT and the results from the full food web simulations. The accordance between EQT and the food web simulations validates the simplifying assumptions behind EQT. EQT provides a "null-solution" to the size- and trait-distributions which may be used as a baseline expectation of the results of large size-structured food web simulations.

[Figure 1 about here.]

2. Food web model

The model is based on a description of the processes of food encounter, growth, reproduction, and mortality at the level of an individual with body mass m (Fig. 1). The model is based on two central assumptions: 1) Prey selection is determined at the individual level where individual predators select prey from the rule "big individuals eat smaller individuals", and at the species level through introduction of species-specific size-independent coupling strengths (Andersen and Ursin, 1977; Werner and Gilliam, 1984; Emmerson and Raffaelli, 2004). 2) In addition to species-specific coupling strengths, species identity is characterised by a single trait: size at maturation m_*. Interactions among individuals are described by a food encounter process which leads to consumption by predators and mortality on their prey. Food consumption leads to growth in body mass, and when an individual reaches size at maturation m_* it starts allocating energy for

reproduction, as well as producing new offspring. Thus the model encapsulates the life-cycle of individuals from birth to maturity and death.

Population dynamics of species i is obtained from individual growth $g_i(m)$ and mortality $\mu_i(m)$ by solving the number conservation equation (McKendrick, 1926; von Foerster, 1959):

$$\frac{\partial N_i}{\partial t} + \frac{\partial}{\partial m}\Big(g_i N_i \Big) = -\mu_i N_i. \tag{1}$$

The population structure of species i is described by the size-spectrum $N_i(m,t)$, denoted $N_i(m)$ to ease notation. The size-spectrum represents the volumetric abundance density distribution of individuals such that $N_i(m)\,dm$ is the number of individuals per unit volume in the mass range $[m;\, m+dm]$. Similarly $B_i(m) = mN_i(m)$ denotes the biomass spectrum (biomass density distribution), and $B_i(m)\,dm$ the biomass per unit volume in the range $[m;\, m+dm]$. The sum of all species' size-spectra plus a resource spectrum $N_R(m)$ is the community spectrum (Fig. 1):

$$N_c(m) = N_R(m) + \sum_i N_i(m). \tag{2}$$

The community spectrum represents the entire biotic environment providing individuals with food (from smaller individuals) as well as their predation risk from larger individuals. To include species-specific preferences each species i has its own *experienced* community spectrum:

$$\mathcal{N}_i(m) = \theta_{i,R} N_R(m) + \sum_j \theta_{i,j} N_j(m), \tag{3}$$

where $\theta_{i,j} \in [0;\, 1]$ is the coupling strength of species i to species j. Coupling strengths are independent of body size (cf. Discussion) since size-dependent food intake is described with a feeding kernel (below).

2.1. Food consumption

The consumption of food by an individual depends on the available food from the experienced community spectrum, on the volume searched per time, and on its functional response. The consumed food is assimilated and used to cover respiratory costs. Remaining available energy is used for somatic growth by immature individuals and for a combination of somatic growth and reproduction by mature individuals.

We incorporate the rule of "big ones eat smaller ones" by assuming that predators have a preferred predator-prey mass ratio (PPMR). This assumption is inspired by stomach analyses of marine fish (Ursin, 1973, 1974), and supported by stable isotope analyses (Jennings et al., 2001). The feeding kernel describing the size preference for prey is prescribed with a normalised log-normal function (Fig. 1, Ursin, 1973):

$$s(m_p, m) = \exp\left[-\left(\ln\left(\frac{\beta m_p}{m} \right) \right)^2 / (2\sigma^2) \right], \tag{4}$$

where m_p is prey mass, m predator mass, β the preferred PPMR, and σ the width of the function. The food available (mass per volume) for a predator of size m is:

$$\phi_i(m) = \int m_p \mathcal{N}_i(m_p) s(m_p, m)\, dm_p. \tag{5}$$

Encountered food (mass per time) is the available food multiplied by the volumetric search rate $v(m) = \gamma m^q$, where q is a positive exponent signifying that larger individuals search a larger volume per unit time (Ware, 1978). Satiation is described using a feeding level (number between 0 and 1, Kitchell and Stewart, 1977; Andersen and Ursin, 1977):

$$f_i(m) = \frac{v(m)\phi_i(m)}{v(m)\phi_i(m) + hm^n}, \tag{6}$$

where hm^n is the maximum food intake. Feeding level times hm^n corresponds to a type II functional response.

2.2. Somatic growth

Ingested food $f(m)hm^n$ is assimilated with an efficiency α accounting for waste products and specific dynamic action. From the assimilated energy an individual has to pay the metabolic costs of standard metabolism and activity, km^p. Thus the energy available for growth and reproduction is:

$$E_i(m) = \alpha f_i(m) hm^n - km^p. \tag{7}$$

Of the available energy a fraction $\psi(m, m_*)$ is used for reproduction, and the rest for somatic growth:

$$g_i(m, m_*) = \begin{cases} \Big(1 - \psi(m, m_*)\Big) E_i(m) & E_i(m) > 0 \\ 0 & \text{otherwise} \end{cases}. \tag{8}$$

If the intake is insufficient to cover respiratory costs ($E_i(m) < 0$) growth is halted. Body size does not shrink when costs cannot be covered, instead starving individuals are exposed to a starvation mortality (see section 2.4). The maximum asymptotic size M an individual can obtain is reached when all available energy is used for reproduction ($\psi(M, m_*) = 1$).

2.3. Reproduction

In order to generate growth trajectories with biphasic growth the allocation rule $\psi(m, m_*)$ has to change smoothly from 0 around size at maturation to 1 at the theoretical maximum asymptotic size M. The allocation rule $\psi(m, m_*)$ is derived using two requirements: 1) that the size of gonads is proportional to individual mass (Blueweiss et al., 1978), and 2) that size at maturation is proportional to asymptotic size (Beverton, 1992; Froese and Binohlan, 2000; He and Stewart, 2001). To obtain an analytical solution as to how individuals allocate available energy to growth and reproduction we assume that the allocation rule is based on a constant feeding level $\overline{f}$. Requiring allocation to reproduction to be proportional to individual mass, $\psi(m, m_*)\overline{E}(m) = k_r m$, gives $\psi(m, m_*) = k_r m / \overline{E}(m)$, where $\overline{E}(m) = \alpha \overline{f} hm^n - km^p$ denotes the available energy when feeding

level is constant. The factor k_r is found by the second requirement through $\psi(M, m_*) = 1$: $k_r = \overline{E}(M)/M$ where $M = m_*/\eta_*$. The allocation can thus be described as:

$$\psi(m, m_*) = \left[1 + \left(\frac{m}{m_*}\right)^{-u}\right]^{-1} \frac{\overline{E}(m_*/\eta_*)}{\overline{E}(m)} \frac{m}{m_*/\eta_*}, \tag{9}$$

where the term in the square brackets is a smooth step function switching from zero to one around the size at maturation (u determines transition width).

The exponents of maximum consumption and standard metabolism are close to equal (cf. Appendix E and Discussion). In the limit of $n = p$ the available energy for growth and reproduction becomes $\overline{E}(m) = \hbar m^n$ where $\hbar = \alpha \overline{f} h - k$. This gives: $\psi(m, m_*) = [1+(m/m_*)^{-u}]^{-1}(\eta_* m/m_*)^{1-n}$, meaning that the juvenile growth pattern is $g = \hbar m^n$ whereas adults grow according to $g = \hbar m^n - \hbar(m_*/\eta_*)^{n-1} m$. Thus the growth model is a biphasic growth model where adults follow von Bertalanffy growth curves as advocated by Lester et al. (2004).

The total flux of offspring is found by integrating the energy allocated to reproduction $\psi(m, m_*)E_i(m)$ over all individual sizes:

$$R_i = \frac{\epsilon}{2m_0} \int N_i(m)\psi(m, m_*)E_i(m)\, dm, \tag{10}$$

where m_0 is the egg size, ϵ the efficiency of offspring production (Appendix C), and 1/2 takes into account that only females spawn (assuming equal sex distribution). Reproduction determines the lower boundary condition of (1) for the size-spectrum of the species:

$$g_i(m_0, m_*)N_i(m_0) = R_i. \tag{11}$$

2.4. Mortality

The mortality rate $\mu(m)$ of an individual has three sources: predation mortality $\mu_p(m)$, starvation mortality $\mu_s(m)$, and a small constant background mortality $\mu_b(m_*)$. The background mortality is needed to ensure that the largest individuals in the community also experience mortality as they are not predated upon by any individuals from the community spectrum.

Predation mortality is calculated such that all that is eaten translates into predation mortalities on the ingested prey individuals (Appendix A):

$$\mu_{p,i}(m_p) = \sum_j \int s(m_p, m)(1 - f_j(m))v(m)\theta_{j,i}N_j(m)\, dm. \tag{12}$$

When food supply does not cover metabolic requirements km^p starvation mortality kicks in. Starvation mortality is proportional to the energy deficiency $km^p - \alpha f(m)hm^n$, and inversely proportional to lipid reserves, which are assumed proportional to body mass:

$$\mu_s(m) = \begin{cases} 0 & E_i(m) > 0 \\ \frac{-E_i(m)}{\xi m} & \text{otherwise} \end{cases}. \tag{13}$$

Mortality from other sources than predation and starvation is assumed constant within a species and inversely proportional to generation time (Peters, 1983):

$$\mu_b = \mu_0 m_*^{n-1}. \tag{14}$$

2.5. Resource spectrum

The resource spectrum $N_R(m)$ represents food items which are needed for the smallest individuals (smaller than βm_0). The dynamics of each size group in the resource spectrum is described using semi-chemostatic growth:

$$\frac{\partial N_R(m,t)}{\partial t} = r_0 m^{p-1}\Big[\kappa m^{-\lambda} - N_R(m,t)\Big] - \mu_p(m) N_R(m,t), \tag{15}$$

where $r_0 m^{p-1}$ is the population regeneration rate (Fenchel, 1974; Savage et al., 2004) and $\kappa m^{-\lambda}$ the carrying capacity. We prefer semi-chemostatic to logistic growth since planktonic resources rebuild from depletion locally due to both population growth and invasions.

[Table 1 about here.]

2.6. Derivation of parameters

Each species is characterised by a single trait, size at maturation m_*, and a species-independent parameter set is achieved through scaling with body size m and m_*. The model is parameterised for marine ecosystems using cross-species analyses of fish communities (Appendix E and Table 1).

The constant γ for the volumetric search rate is difficult to assess (Appendix E). However, since the feeding level $f(m)$ of small individuals is determined solely by the amount of encountered food from the resource spectrum, we may use *initial feeding level* f_0 as a physiological measure of food encounter; f_0 is defined as the feeding level resulting from a resource spectrum at carrying capacity. The initial feeding level is used as a control parameter for food availability (enrichment), through which the value of γ can be calculated (Appendix D):

$$\gamma_i(f_0) = \frac{f_0 h \beta^{2-\lambda}}{(1-f_0)\sqrt{2\pi}\theta_{i,R}\kappa\sigma}, \tag{16}$$

where it is noted that γ will be species dependent if species have different coupling strengths to the resource.

A *critical feeding level* f_c can be formulated as the feeding level where all assimilated food is used for metabolic costs (using values from Table 1):

$$f_c = \frac{k}{\alpha h} m^{p-n} = \frac{k}{\alpha h} \approx 0.2. \tag{17}$$

Individuals can only grow and reproduce if $f > f_c$. Assuming that individuals experience an average feeding level $\overline{f}$, the growth (8) of juveniles is $g = \hbar m^n$ (for $n = p$). The parameter $\hbar = \alpha h \overline{f} - k$ can be estimated through the relation between observed von Bertalanffy growth rate and asymptotic size yielding $\hbar \approx 10\,\mathrm{g}^{0.25}$/year (Andersen et al., 2008). This allows an estimation of the expected average feeding level of individuals in the field (Table 1):

$$\overline{f} = \frac{\hbar + k}{\alpha h} \approx 0.4, \tag{18}$$

i.e. around twice the critical feeding level. As the initial feeding level f_0 is calculated from a resource spectrum at carrying capacity, the realised feeding level in the model will be smaller than f_0. A value of $f_0 = 0.6$ was seen to give realised feeding levels around 0.4.

3. Methods

Stable food webs are constructed using the full dynamic food web model with random coupling strengths $\theta_{i,j}$. For each run, 30 species are assigned with m_* evenly distributed on a logarithmic size axis ($m_* \in [0.25\,\mathrm{g};\, 20\,\mathrm{kg}]$), random $\theta_{i,j}$ matrices (mean 0.5), and a common $\theta_{i,R} = 0.5$ coupling to the resource spectrum. Numerical integration is performed by standard finite difference techniques (Appendix G). Food webs are simulated in 10 consecutive intervals covering 300 years each, where species with a biomass less than $10^{-30}\mathrm{g/m}^3$ are eliminated after each interval. To eliminate food webs that still have not reached the final state each community is integrated for additional 500 years and discarded if any species has an absolute population growth rate larger than 1 logarithmic decade per 100 years. To ensure that each food web in the final ensemble spans multiple trophic levels we only retain food webs where at least one species has m_* larger than 2.5 kg. For statistics we use the mean of the last 250 years of the simulation with time steps saved in 0.1 year increments. In this manner 204 food webs having a total number of 1016 species were collected. Each web contained between 2 and 9 species with a mean of 4.98 species.

We analyse the generated food webs in terms of distributions of average community size-spectrum, species size-spectra, trait biomass distributions, and trait diversity distributions. Additionally we demonstrate the importance of distinguishing between what an individual prefers to eat and what is actually ingested (i.e. found in its stomach) by showing how emerging PPMRs vary with food availability and differ from preferred PPMRs.

An approximate steady-state solution to the food web model which neglects the dynamics of reproduction can be found using two assumptions: 1) all species consume food and experience mortality from a scaling community size-spectrum $N_c = \kappa_c m^{-\lambda}$, and 2) constant feeding level $\overline{f}$, which implies equal species coupling strengths $\theta_{i,j} = \overline{\theta}$. Whereas the food webs in the full model are based on a discrete set of m_*, the analytical solution considers m_* as a continuous distribution. The procedure for deriving the analytical solution is similar to the derivation of equilibrium size-spectrum theory (Andersen and Beyer, 2006), but the results are slightly different as standard metabolism is taken explicitly into account here. The food encountered by an individual is found using assumption 1): $v(m)\phi(m) = \gamma m^q \int N_c s(m_p, m) m_p \, dm_p \propto m^{2-\lambda+q}$. The feeding level is calculated from (6), and the requirement that it is constant (assumption 2) leads to a constraint on the exponent of the community spectrum: $\lambda = 2 + q - n$. Feeding with a constant feeding level generates a predation mortality of $\mu_p = \alpha_p m^{n-1}$ (Appendix A). The size-spectrum of juvenile individuals is found as the steady state solution of (1) using the above predation mortality and $g = \hbar m^n$ (cf. (F.1)): $N(m, m_*) = \kappa(m_*) m^{-n-a}$, where $a = \alpha_p/\hbar$ is the physiological level of predation (Beyer, 1989; Andersen and Beyer, 2006), which can be calculated as $a \approx \overline{f}/(\overline{f} - f_c)\beta^{2n-q-1}/\alpha = 0.86$ (Appendix B). The constant $\kappa(m_*)$ is found from the requirement that the sum of all species spectra should equal the community spectrum. Assuming a continuum of species the requirement can be written as $\int N(m, m_*)\, \mathrm{d}m_* = N_c(m)$ which leads to $\kappa(m_*) \propto m_*^{2n-q-3+a}$ (Fig. 1). This approximate solution of the model will be referred to as equilibrium size-spectrum

theory (EQT), and it will be compared to the output of the complete dynamic food web model.

In dynamic models, as in nature, the lifetime reproductive success (fitness) has to be $R_0 = 1$ for all coexisting species. Since EQT does not consider the boundary condition (11) life-time reproductive success becomes a function of size at maturation: $R_0 \propto m_*^{1-a}$ (Andersen et al., 2008). One solution to making R_0 independent of m_* is to set $a = 1$, but that breaks the above employed mass balance between growth and mortality used to calculate a. Due to the $R_0 \neq 1$ inconsistency in EQT we have a specific focus on the realised values of a when comparing food web simulations with EQT predictions. To examine how the regulation of R_0 occurs in the full food web model R_0 is split into two factors: 1) the probability of surviving to become adult, and 2) lifetime reproduction per adult (Appendix F):

$$p_{m_0 \to m} = \frac{N(m)g(m, m_*)}{N(m_0)g(m_0, m_*)}, \tag{19}$$

$$R_{\text{adult}}(m_*) = \int_{m_*}^{M} p_{m_* \to m} \frac{\psi(m, m_*)E(m)}{g(m, m_*)} dm. \tag{20}$$

Survival probabilities and reproductive outputs in the food web simulations are compared with EQT predictions, which are calculated by inserting the EQT size-spectra into (19) and (20). Juvenile growth is $g \propto m^n$, which gives $p_{m_0 \to m_*} \propto m_*^{-n-a} m_*^n = m_*^{-a}$ and $R_{\text{adult}} \propto m_*$.

[Figure 2 about here.]

4. Model predictions

4.1. Growth trajectories

In unstructured models fluctuations are manifested as oscillations in the biomass of species, whereas the oscillations in structured models stem from oscillations in the size-spectrum composition. Such oscillations give rise to fluctuating feeding levels as individuals encounter different levels of food in different life-stages (Fig. 2.a). Variations in feeding levels between species and as a function of individual size lead to different emergent growth trajectories (Fig. 2.b). The growth trajectories roughly follow the biphasic growth curve that is obtained if the feeding level is assumed to be constant.

[Figure 3 about here.]

[Figure 4 about here.]

4.2. Biomass structure

By pooling species from each food web into logarithmic evenly distributed m_* groups, and summing the size-spectra in each group, a size-spectrum is obtained for each m_* group. Next, the logarithmic average of m_* groups across all food webs is performed to produce the average size-spectra of a m_* group (Fig. 3). Average community biomass spectrum $N_c(m)m$ follows the

EQT prediction of a slope of $1 + q - n = 1.05$, meaning that the biomass in logarithmically evenly sized size-groups, $\int_m^{cm} N_c(m)mdm$, is a slightly declining function of body mass. The community spectrum oscillates around the EQT prediction due to a trophic cascade initiated by a superabundance of the largest predators which do not experience any predation mortality (Andersen and Pedersen, 2010). The peaks of the oscillating pattern are roughly spaced by the preferred PPMR. Biomass density within species is constant until individuals reach the end of the resource spectrum, and larger individuals, $\gtrsim 0.1\,\mathrm{g}$, have a biomass spectrum slope flatter than that of the community spectrum (Fig. 3). Thus, in contrast to EQT, the dynamic model produces species size-spectra that cannot be described as power laws. The number of small individuals is inversely related to size at maturation. The scaling of offspring abundance can be calculated using EQT as $N_0 \propto \int_{m_*}^{cm_*} \kappa(m'_*)dm'_* \propto m_*^{2n-q-2+a}$, which fits the simulated results well for $a = 1$ (Fig. 3, inset).

The distribution of species biomass as a function m_* can be calculated from EQT as:

$$B(m_*) = \int_{m_*}^{cm_*} \int_{m_0}^{M} N(m, m'_*)mdm\, dm'_* \propto m_*^{n-q}. \tag{21}$$

As n and q are almost equal the biomass distribution $B(m_*)$ as a function of m_* is almost constant. This result is also borne out by the dynamical simulations (Fig. 4.a) with some variation due to uneven species distribution along the m_* axis: peaks occur in species diversity separated by the preferred PPMR β (Fig. 4.b).

[Figure 5 about here.]

4.3. PPMR and feeding level

The realised mean PPMR can be derived when prey concentrations are known: $\mathcal{N}(m_p)s(m_p, m)$ is the prey size distribution encountered by a m sized predator. Mean prey size encountered by a m sized predator is $\frac{\int_0^\infty m_p \mathcal{N}(m_p)s(m_p,m)dm_p}{\int_0^\infty \mathcal{N}(m_p)s(m_p,m)dm_p}$. The realised mean PPMR is calculated as the predator size m divided by the mean prey size:

$$PPMR(m) = \frac{m\int_0^\infty \mathcal{N}(m_p)s(m_p, m)dm_p}{\int_0^\infty m_p\mathcal{N}(m_p)s(m_p, m)dm_p}. \tag{22}$$

Realised mean PPMR is always larger than the preferred PPMR β, due to higher abundance of smaller prey items (Fig. 5.a). The realised mean PPMR calculated from EQT (using $\mathcal{N} \propto m_p^{-\lambda}$) is $\exp[(\lambda - 3/2)\sigma^2]\beta \approx 1.7\beta$. Realised PPMR from the simulations oscillate around this value due to the fluctuations in the community spectrum (Fig. 3).

As individuals grow to a size larger than βm_0 they switch from eating food in the resource spectrum to feeding on other species. This leads to a decrease in the feeding level from $f_0 = 0.6$ to about 0.45. The oscillations in feeding level increase in magnitude as body size increases due to larger fluctuations in prey availability (Fig. 5.b). Many large individuals periodically have a feeding level below the critical feeding level f_c (where starvation kicks in) since prey items in the

preferred size range become scarce, which results in ingestion of smaller food items and therefore increasing PPMR.

[Figure 6 about here.]

4.4. Reproduction and survival

Lifetime adult reproduction calculated from the simulated food webs fit the EQT prediction since it scales linearly with m_* (Fig. 6.b). The probability of surviving to a given size is independent of m_*, as the survival curves of the different m_* groups lie on top of one another (Fig. 6.a). Survival to m_* scales inversely with m_* (i.e. $a = 1$, crosses in Fig. 6.a), which ensures that R_0 is constant. However, if the $a = 1$ scaling of survival to m_* is extrapolated to m_0 it is seen that it does not intersect $p_{m_0 \to m_0} = 1$. Instead the survival curves change slope between m_0 and around 10^{-1} g where predation mortality starts to dominate due to an abundance of fish individuals in the same order of magnitude as the resource spectrum, which is intensified by reduced growth stemming from food competition (Fig. 3). In summary survival does not scale with m_*^{-a} as predicted by EQT. Instead adult survival scales with m_*^{-1} (i.e. $a = 1$) whereas individuals smaller than ≈ 0.1 g have a higher survival (i.e. a smaller scaling exponent).

5. Discussion

We have developed a generic food web framework suitable for analysing systems of interacting size-structured populations. The framework increases ecological realism compared to traditional unstructured food web models by explicitly resolving the whole life-history of individuals, but maintains simplicity by describing species with only one trait: maturation size m_*. Remaining parameters are made species-independent through inter- and intraspecies scaling with m_* and body mass m. The productivity of the system is characterised by one parameter, the initial feeding level f_0. Feeding behaviour is assumed to be determined by a feeding kernel with a fixed preferred PPMR (big individuals eat small individuals), multiplied by a species-specific coupling strength.

Only characterising the life-history and feeding preference of individuals of a species by body mass m and trait m_* is clearly a simplification, but contemporary knowledge suggests that a large part of the individual bioenergetics related to growth (Peters, 1983) and reproduction (Blueweiss et al., 1978) indeed can be described by such scaling. Additionally it is well-known that predators often outsize their prey (Brose et al., 2006a) which justifies the use of the generalisation "big ones eat small ones".

5.1. Model architecture

The model was parameterised from cross-species analyses of fish communities, since aquatic systems constitute a group of strongly size-structured ecosystems. Other less strongly size-structured

taxa can be modelled as well through reparametrisation and by allowing each species to have its own offspring size $m_{0,i}$. Additionally, the description of how available energy energy is divided between growth and reproduction may have to be reformulated since animals in other taxa may exhibit determinate growth. Determinate growth can be modelled simply by replacing the allocation function (9) with only the part within the square brackets.

The proposed modelling framework is similar to physiologically structured models (Andersen and Ursin, 1977; Metz and Diekmann, 1986; de Roos and Persson, 2001), and as these based on mechanistic individual-level processes. Our contribution is to employ a trait-based description of species identity, and a formulation of food preference which is split into a size- and a species-based contribution, which renders the developed framework useful as a generic food web framework. Recently the PSPM approach has been reduced to a stage-structured model which facilitates multi-species studies (de Roos et al., 2008a); however this is achieved at the cost of collapsing continuous size-structure to a discrete stage-structure. A first step towards multi-species PSPMs was carried out with an intra-guild predation model, which showed that obtaining species coexistence between two size-structured populations is a difficult task (van de Wolfshaar et al., 2006); a result which is probably due to insufficient ecological differentiation of the two species. In the proposed framework the trait maturation size provides a simple and logical way of representing ecological differentiation of species, whereas this differentiation in PSPMs is less clear due to large species-specific parameter sets. Additional ecological differentiation and heterogeneity are obtained by also including food web structure in the form of species coupling strengths.

An alternative approach to model a size-structured community is the community size-spectrum models (Silvert and Platt, 1980; Benoît and Rochet, 2004). In these models the community is represented by a community size-spectrum of all individuals irrespective of species identity (Sheldon and Parsons, 1967). As with the physiologically structured models these are based on individual-level descriptions of life-history. The community spectrum approach has the drawback that species are not resolved, as all individuals are lumped together into one spectrum. Their advantage is their ability to make community-wide predictions with simple means (Blanchard et al., 2009) similarly to the mean-field theory in unstructured food webs (McKane et al., 2000; Wilson et al., 2003).

A central element in the model is the division of energy between somatic growth and reproduction through the allocation function $\psi(m, m_*)$. As in PSPMs our bioenergetic model is a net-production model where it is assumed that metabolic costs are covered with highest priority after which the remaining energy can be used for growth and reproduction. PSPMs are formulated either with one state variable: individual body weight (Kooijman and Metz, 1984; Claessen and de Roos, 2003), or with two state variables: somatic weight and reserve weight (de Roos and Persson, 2001). In the latter case energy is divided between the two states such that the ratio between the two state variables is aimed to be constant, and accumulated reserves are used for reproduction at the end of the growing season. In the case with only one state variable surplus energy is divided between somatic growth and reproduction with a fixed ratio (κ-rule). When us-

ing the κ-rule the maximum asymptotic size any species individual can obtain is M_+ where intake $\alpha h f(M_+) M_+^n$ equals the metabolic costs $k M_+^p$ – meaning that all species would obtain the same asymptotic size if parameters are species independent as in our formulation. M_+ is very sensitive to the precise values of n and p, and they can therefore only be regarded as poor determinators for asymptotic size (Andersen et al., 2008). Our model deviates from the single-state PSPMs in this partitioning of energy, as we assume that mature individuals allocate an amount proportional to their body size for reproduction (Blueweiss et al., 1978), and that asymptotic size depends on the trait size at maturation (Beverton, 1992; Froese and Binohlan, 2000; He and Stewart, 2001). This ensures that the ratio between gonad size and somatic weight is constant within a species, which is similar to the partitioning rule used in two-state PSPMs. The allocation function is derived under the assumption of a constant feeding level throughout adult life. Even though the feeding level is assumed constant, the actual allocation still vary depending on the actual food availability, as $\psi(m, m_*)$ only determines the fraction of available energy allocated to reproduction. An alternative way to derive $\psi(m, m_*)$ is to let it depend on actual feeding levels. This assumption, however, would imply that individuals adjust their allocation to reproduction such that asymptotic size is always reached. This does not seem plausible as individuals in resource scarce environments probably obtain smaller maximum sizes, and therefore we find the most reasonable assumption to be that of a constant feeding level. The exponents n and p are close to equal in nature, and for $n = p$ the energy allocation function leads to biphasic growth where adults follow von Bertalanffy growth curves (Lester et al., 2004). We fixed the yearly mass-specific allocation to reproduction (yearly gonado-somatic index, GSI) to be independent of individual body size within a species. The obtained form of $\psi(m, m_*)$, however, yields a m_*^{n-1} scaling of yearly GSI across species, which is consistent with empiric evidence (Gunderson, 1997). This means that the form of $\psi(m, m_*)$ implies a trade-off between m_* and the mass-specific reproduction: large m_* species can escape predation mortality via growth by paying the price of a lower mass-specific reproduction (Charnov et al., 2001). When the exponents n and p differ, growth will still be biphasic and adult growth curves will be similar to von Bertalanffy curves (see also Andersen and Pedersen, 2010). In conclusion the derived allocation rule leads to realistic growth patterns.

5.2. Food web structure

Food web structure is the most essential part of a food web model, and in principle two approaches can be taken to obtain a structure for a dynamic food web model: a top-down and a bottom-up approach.

The top-down method generates food web matrices from the desired number of species and connectance using a static model (stochastic phenomenological models: Cohen and Newman (1985); Williams and Martinez (2000); Cattin et al. (2004); Allesina et al. (2008), or more mechanistic approaches involving phylogenetic correlations (Rossberg et al., 2006) or foraging theory (Petchey et al., 2008)). Next, the food web matrix is used to drive a dynamic model, which is simulated

forward in time where some of the initial species will go extinct, and the remaining species set can be used for analysis. Note that in addition to a decreased species richness in the final community other food web statistics as e.g. the final connectance may differ as well (Uchida and Drossel, 2007).

In the bottom-up approach link strengths are determined from ecological relations, such as e.g. a predator-prey feeding kernel: if the prey fits into a certain size range relative to the predator size, then interaction occurs between the nodes with a strength determined by the feeding kernel (Loeuille and Loreau, 2005; Virgo et al., 2006; Lewis and Law, 2007). Predator preferences depend, in addition to ecological characters, on evolutionary history and recent approaches add this component of phylogenetic correlations (Rossberg et al., 2008).

For size-structured food webs a top-down algorithm for generating realistic food web matrices does not exist. This is due to lack of data describing the three dimensional interaction matrix – dimension one and two is respectively predator and prey identity as in the classic interaction matrix, and the third dimension is predator/prey body size. Thus one is confined to the bottom-up approach and/or random interaction matrices. In this study we use the bottom-up approach to prescribe interactions to obey the pattern of "big ones eat smaller ones". Life-history omnivory (Pimm and Rice, 1987) is therefore naturally incorporated in size-structured food webs through the use of a feeding kernel. To obtain an ensemble of different communities we use the top-down approach of a classical two-dimensional predator-prey interaction matrix – that is we assume that regardless of size individuals within a species have equal potential maximum link strength (coupling strengths in our model) to another species. As no top-down method exists for generating this matrix we use random matrices. The actual link strength is the product of the coupling strength and the feeding kernel, meaning that link strengths indeed are dynamic as they depend on the size-structure of both prey and predator.

As we generate food webs from a fixed initial pool of only 30 species and use a random matrix as coupling matrix we only obtain small food webs (maximum: 9 species). However, it should be noted that the number of resource species the resource spectrum represents is not included. To obtain larger food webs a larger species pool is needed along with a sequential assembly algorithm (Post and Pimm, 1983), and a better method for obtaining coupling strengths between species. Our primary interest in the food web analyses has been the size- and trait-structure of food webs with a finite number of species, and how these compare with EQT predictions, which are based on the premise of a continuum of species. The general correspondence with EQT indicates that the broad-scale patterns are relatively insensitive to how the species-specific coupling strengths (i.e. food web structure) are specified. Still, an interesting follow-up study would be focused on the coupling matrix structure, which may more generally be size-dependent, and how the effective food web structure that emerges from the coupling strengths and feeding kernel compares with empiric food webs.

5.3. Community structure

We generated an ensemble of size-structured food webs and used averages over these to make general predictions of the structure of fish communities, in particular the size-structure of individual populations, and how these spectra "stack" to form the community size-spectrum. In accordance with EQT we find the community spectrum to scale with $\lambda = 2 + q - n \approx 2$ meaning that the distribution of biomass as a function of individual body size is close to constant when individuals are sorted into logarithmically evenly sized bins. This prediction means that the biomass of individuals between e.g. 1 g and 10 g is the same as those present with body sizes between 1 kg and 10 kg, in accordance with the Sheldon hypothesis (Sheldon et al., 1972).

The distribution of biomass as a function of m_* is predicted to be almost independent of m_* in accordance with EQT. The result is reminiscent of the Sheldon hypothesis, and it can be formulated as an extension of the Sheldon hypothesis: *"The total biomass of individuals ordered in logarithmically spaced groups of their maturation size is approximately constant"*. This means that the total biomass of all species with m_* between 1 and 10 g is approximately the same as that of species with m_* within 1 to 10 kg. This prediction is a novel extension and could be tested by size-based field data. In contrast to EQT the dynamic framework also provides predictions on the distribution of the number of species as a function of m_*. Species tend to cluster in groups on the m_* axis separated by a distance corresponding to the preferred PPMR β. This clustering is partly a reflection of the use of a fixed value of β; more diversity in feeding strategies (i.e. different β) would probably smoothen the species distribution as well as making the feeding level more constant.

The size-spectra of individual species do not to follow power laws as predicted by EQT since there is a change in spectrum slopes from small to medium sized individuals. This difference stems from different scaling relationships for the survival probability of small and larger individuals. The less steep slope in survival for small individuals is due to a proportionally low mortality rate caused by their low abundance relative to similarly sized resource items. Incorporating mortality from the resource spectrum on the smallest individuals may thus result in a single survival probability scaling. The probability of surviving to m_* scale as m_*^{-a} for a physiological predation constant value of $a = 1$, which is conflicting with the value $a = 0.86$ predicted by EQT. The discrepancy about the value of a highlights an inconsistency within EQT: Enforcement of mass-balance between growth and predation leads to $a = 0.86$, while the reproductive boundary condition can only be fulfilled if $a = 1$. The full food web simulations demonstrate that both the scaling of surviving to m_* and the scaling of the number of offspring are best predicted by a value of $a = 1$. This indicates that when EQT predictions depend on a, the value $a = 1$ should be used even though that breaks mass conservation in EQT.

Lastly we demonstrate that realised PPMRs (i.e. PPMRs based on ingested prey) emerge in the model. Average realised PPMR is always larger than the preferred PPMR β since smaller prey items are more abundant than larger ones. It is found that the realised PPMR is proportional

to the preferred ratio ($PPMR = 1.7\beta$). Model predictions show that realised PPMR oscillates around this value due to fluctuations in the average community spectrum. PPMR displays large fluctuations with size demonstrating that determination of PPMR from single measurements is problematic due to high prey abundance sensitivity. Empirical findings show that realised PPMRs increase with body size (Barnes et al., 2010), but one should be careful about concluding that the preferred PPMR (which we put into models) shares this size scaling, since relative abundances may cause the increase rather than actual behavioural prey preferences: even though we have a fixed preferred PPMR our model predicts that realised PPMR is an increasing function of body size.

5.4. Conclusion and outlook

The proposed food web framework increases ecological realism in food web models as it resolves the complete life-history of individuals by representing the size-structure of each species with a size-spectrum. More specifically the framework complies with five requirements of (cf. Introduction): 1) being generic with few parameters, 2) being mechanistic and utilising individual-level processes, 3) including food dependent growth, 4) being practically solvable for species-rich communities, and 5) complying with data on community structure and individual growth curves.

Trait-based size-structured food webs can be examined at four levels of organisation: at community level, at species level, at trait level, and at the individual level. We generated empirically testable hypotheses of mainly biomass distributions at different levels of organisation.

By assuming a power law community spectrum and a constant feeding level the full dynamic model can be simplified to an EQT model (Andersen and Beyer, 2006). Correspondence of predictions by EQT and the full model justifies the use of the simplifying assumptions. EQT is a powerful analytical tool that in a simple manner yields insight to e.g. the biomass distributions within and across species in size-structured food webs. However, as EQT assumes steady-state, the study of emerging effects, e.g. diversity and responses to perturbations, has to be conducted with the full model.

The PSPM framework has showed existence of alternative stable states where single populations can exist with different size-structure compositions (de Roos and Persson, 2002; Persson et al., 2007; de Roos et al., 2008b). It is an open question whether such alternative states become more widespread or if they disappear when more species interact with each other. This question is important since it tells whether such alternative states are expected to occur frequently or rarely in nature, and consequently whether exploitation can easily induce shifts between states. An important future challenge is thus to study the possibilities of multiple states in complex food webs – not only of single individual populations, but of the ecosystem as a whole. The proposed framework allows exactly this kind of studies since it provides a full ecologically realistic but conceptually simple model of size-structured ecosystems.

Natural future extensions of the model could be to allow the species coupling strengths to

be size-dependent and make coupling strengths depend on vulnerability and forageability of prey and predators (Rossberg et al., 2008) as well as on the spatial overlaps of the interacting species. Adding this extra level of mechanistic realism would allow the framework to be useful for studying ecosystem consequences of spatial changes of species populations, which could be driven by climatic changes.

Acknowledgements

Niels Gerner Andersen is thanked for valuable discussions on bioenergetic models. MH was supported by the European Marie Curie Research Training Network FishACE (Fisheries-induced Adaptive Changes in Exploited Stocks) funded through the European Community's Sixth Framework Programme (Contract MRTN-CT-2004-005578). KHA was supported by the EU 7th framework research projects MEECE and FACTS.

References

Allesina, S., Alonso, D., Pascual, M., 2008. A general model for food web structure. Science 320, 658.

Andersen, K.H., Beyer, J.E., 2006. Asymptotic size determines species abundance in the marine size spectrum. The American Naturalist 168, 54–61.

Andersen, K.H., Beyer, J.E., Pedersen, M., Andersen, N.G., Gislason, H., 2008. Life-history constraints on the success of the many small eggs reproductive strategy. Theoretical Population Biology 73, 490–497.

Andersen, K.H., Pedersen, M., 2010. Damped trophic cascades driven by fishing in model marine ecosystems. Proc. R. Soc. B 277, 795–802.

Andersen, K.P., Ursin, E., 1977. A Multispecies Extension to the Beverton and Holt Theory of Fishing, with Accounts of Phosphorus Circulation and Primary Production. Meddelelser fra Danmarks Fiskeri- og Havundersgelser, N.S 7, 319–435.

Barnes, C., Maxwell, D., Reuman, D.C., Jennings, S., 2010. Global patterns in predator-prey size relationships reveal size dependency of trophic transfer efficienc. Ecology 91, 222–232.

Benoît, E., Rochet, M.J., 2004. A continuous model of biomass size spectra governed by predation and the effects of fishing on them. Journal of Theoretical Biology 226, 9–21.

Beverton, R., 1992. Patterns of reproductive strategy parameters in some marine teleost fishes. Journal of Fish Biology 41, 137–160.

Beyer, J.E., 1989. Recruitment stability and survival – simple size-specific theory with examples from the early life dynamics of marine fish. Dana 7, 45–147.

Blanchard, J.L., Jennings, S., Law, R., Castle, M.D., McCloghrie, P., Rochet, M.J., Benot, E., 2009. How does abundance scale with body size in coupled size-structured food webs? Journal of Animal Ecology 78, 270–280.

Blueweiss, L., Fox, H., Kudzma, V., Nakashima, D., Peters, R., Sams, S., 1978. Relationships between Body Size and Some Life History Parameters. Oecologia (Berl.) 37, 257–272.

Boudreau, P.R., Dickie, L.M., 1992. Biomass Spectra of Aquatic Ecosystems in Relation to Fisheries Yield. Can. J. Fish. Aquat. Sci. 49, 1528–1538.

Brose, U., Jonsson, T., Berlow, E.L., Warren, P., Banasek-Richter, C., Bersier, L.F., Blanchard, J.L., Brey, T., Carpenter, S.R., Blandenier, M.F.C., Cushing, L., Dawah, H.A., Dell, T., Edwards, F., Harper-Smith, S., Jacob, U., Ledger, M.E., Martinez, N.D., Memmott, J., Mintenbeck, K., Pinnegar, J.K., Rall, B.C., Rayner, T.S., Reuman, D.C., Ruess, L., Ulrich, W., Williams, R.J., Woodward, G., Cohen, J.E., 2006a. Consumer-resource body-size relationships in natural food webs. Ecology 87, 2411–2417.

Brose, U., Williams, R.J., Martinez, N.D., 2006b. Allometric scaling enhances stability in complex food webs. Ecology Letters 9, 1228–1236.

Cattin, M.F., Bersier, L.F., Banašek-Richter, C., Baltensperger, R., Gabriel, J.P., 2004. Phylogenetic constraints and adaptation explain food-web structure. Nature 427, 835–839.

Charnov, E.L., Turner, T.F., Winemiller, K.O., 2001. Reproductive constraints and the evolution of life histories with indeterminate growth. PNAS 98, 9460–9464.

Claessen, D., de Roos, A.M., 2003. Bistability in a size-structured population model of cannibalistic fish - a continuation study. Theoretical Population Biology 64, 49–65.

Cohen, J.E., Newman, C.M., 1985. A stochastic theory of community food webs: I. models and aggregated data. Proc. R. Soc. Lond. B 224, 421–448.

Daan, N., Gislason, H., Pope, J.G., Rice, J.C., 2005. Changes in the North Sea fish community: evidence of indirect effects of fishing? ICES Journal of Marine Science 62, 177–188.

Emmerson, M., Raffaelli, D., 2004. Predator-prey body size, interaction strength and the stability of a real food web. Journal of Animal Ecology 73, 399–409.

Fenchel, T., 1974. Intrinsic Rate of Natural Increase: The Relationship with Body Size. Oecologia 14, 317–326.

von Foerster, H., 1959. Some Remarks on Changing Populations, in: Stohlman, F. (Ed.), The Kinetics of Cellular Proliferation. Grune & Stratton, pp. 382–407.

Froese, R., Binohlan, C., 2000. Empirical relationships to estimate asymptotic length, length at first maturity and length at maximum yield per recruit in fishes, with a simple method to evaluate length frequency data. Journal of Fish Biology 56, 758–773.

Gunderson, D.R., 1997. Trade-off between reproductive effort and adult survival in oviparous and viviparous fishes. Can. J. Fish. Aquat. Sci. 54, 990–998.

He, J.X., Stewart, D.J., 2001. Age and size at first reproduction of fishes: predictive models based only on growth trajectories. Ecology 82, 784–791.

588 Jennings, S., Greenstreet, S., Hill, L., Piet, G., Pinnegar, J., Warr, K., 2002. Long-term trends in the trophic structure of the North Sea fish community: evidence from stable-isotope analysis, size-spectra
590 and community metrics. Marine Biology 141, 1085–1097.

Jennings, S., Pinnegar, J.K., Polunin, N.V.C., Boon, T.W., 2001. Weak cross-species relationships between
592 body size and trophic level belie powerful size-based trophic structuring in fish communities. Journal of Animal Ecology 70, 934–944.

594 Kitchell, J.F., Stewart, D.J., 1977. Applications of a Bioenergetics Model to Yellow Perch (Perca flavescens) and Walleye (Stizostedion vitreum vitreum). J. Fish. Res. Board Can. 34, 1922–1935.

596 Kooijman, S.A.L.M., Metz, J.A.J., 1984. One the Dynamics of Chemically Stressed Populations: The Deduction of Population Consequences from Effects on Individuals. Ecotoxicology and Environmental
598 Safety 8, 254–274.

Lester, N.P., Shutter, B.J., Abrams, P.A., 2004. Interpreting the von Bertalanffy model of somatic growth
600 in fishes: the cost of reproduction. Proc. R. Soc. Lond. B. 271, 1625–1631.

Lewis, H.M., Law, R., 2007. Effects of dynamics on ecological networks. Journal of Theoretical Biology
602 247, 64–76.

Loeuille, N., Loreau, M., 2005. Evolutionary emergence of size-structured food webs. PNAS 102, 5761–
604 5766.

McKane, A., Alonso, D., Sole, R., 2000. Mean-field stochastic theory for species-rich assembled communi-
606 ties. Physical Review E 62, 8466–8484.

McKendrick, A.G., 1926. Applications of Mathematics to Medical Problems. Proceedings of the Edinburgh
608 Mathematical Society 44, 98–130.

Metz, J.A.J., Diekmann, O. (Eds.), 1986. The Dynamics of Physiologically Structured Populations. vol-
610 ume 68 of *Lecture Notes in Biomathematics*. Springer-Verlag.

Persson, L., Amundsen, P.A., de Roos, A.M., Klemetsen, A., Knudsen, R., Primicerio, R., 2007. Culling
612 Prey Promotes Predator Recovery – Alternative States in a Whole-Lake Experiment. Science 316, 1743–1746.

614 Petchey, O.L., Beckerman, A.P., Riede, J.O., Warren, P.H., 2008. Size, foraging, and food web structure. PNAS 105, 4191–4196.

616 Peters, R.H., 1983. The ecological implications of body size. Cambridge University Press.

Pimm, S., Rice, J., 1987. The dynamics of multispecies, multi-life-stage models of aquatic food webs.
618 Theoretical population biology 32, 303–325.

Post, W., Pimm, S., 1983. Community assembly and food web stability. Mathematical Biosciences 64,
620 169–182.

de Roos, A.M., Persson, L., 2001. Physiologically structured models – from versatile technique to ecological
622 theory. Oikos 94, 51–71.

de Roos, A.M., Persson, L., 2002. Size-dependent life-history traits promote catastrophic collapses of top predators. PNAS 99, 12907–12912.

de Roos, A.M., Schellekens, T., Kootenb, T.V., Wolfshaar, K.V.D., Claessen, D., Persson, L., 2008a. Simplifying a physiologically structured population model to a stage-structured biomass model. Theoretical Population Biology 73, 47–62.

de Roos, A.M., Schellekens, T., Van Kooten, T., Persson, L., 2008b. Stage-specific predator species help each other to persist while competing for a single prey. PNAS 105, 13930–13935.

Rossberg, A., Ishii, R., Amemiya, T., Itoh, K., 2008. The top-down mechanism for body-mass-abundance scaling. Ecology 89, 567–580.

Rossberg, A., Matsuda, H., Amemiya, T., Itoh, K., 2006. Food webs: experts consuming families of experts. Journal of Theoretical Biology 241, 552–563.

Savage, V.M., Gillooly, J.F., Brown, J.H., West, G.B., Charnov, E.L., 2004. Effects of Body Size and Temperature on Population Growth. The American Naturalist 163, 429–441.

Sheldon, R.W., Parsons, T.R., 1967. A Continuous Size Spectrum for Particulate Matter in the Sea. J. Fish. Res. Board Can. 24, 909–915.

Sheldon, R.W., Prakash, A., Sutcliffe, Jr., W.H., 1972. The size distribution of particles in the ocean. Limnology and Oceanography 17, 327–340.

Silvert, W., Platt, T., 1980. Dynamic Energy-Flow Model of the Particle Size Distribution in Pelagic Ecosystems, in: Kerfoot, W.C. (Ed.), Evolution and Ecology of Zooplankton Communities. The University Press of New England, pp. 754–763.

Uchida, S., Drossel, B., 2007. Relation between complexity and stability in food webs with adaptive behavior. Journal of Theoretical Biology 247, 713–722.

Ursin, E., 1973. On the Prey Size Preferences of Cod and Dab. Meddelelser fra Danmarks Fiskeri- og Havundersgelser, N.S 7, 85–98.

Ursin, E., 1974. Search Rate and Food Size Preference in Two Copepods. ICES CM L/23, 1–13.

Ursin, E., 1982. Stability and variability in the marine ecosystem. Dana 2, 51–67.

Virgo, N., Law, R., Emmerson, M., 2006. Sequentially assembled food webs and extremum principles in ecosystem ecology. Journal of Animal Ecology 75, 377–386.

Ware, D.M., 1978. Bioenergetics of Pelagic Fish: Theoretical Change in Swimming Speed and Ration with Body Size. J. Fish. Res. Board. Can. 35, 220–228.

Werner, E.E., Gilliam, J.F., 1984. The Ontogenetic Niche and Species Interactions in Size-Structured Populations. Ann. Rev. Ecol. Syst. 15, 393–425.

Williams, R.J., Martinez, N.D., 2000. Simple rules yield complex food webs. Nature 404, 180–183.

Wilson, W., Lundberg, P., Vázquez, D., Shurin, J., Smith, M., Langford, W., Gross, K., Mittelbach, G., 2003. Biodiversity and species interactions: extending Lotka-Volterra community theory. Ecology Letters 6, 944–952.

van de Wolfshaar, K.E., de Roos, A.M., Persson, L., 2006. Size-Dependent Interactions Inhibit Coexistence in Intraguild Predation Systems with Life-History Omnivory. The American Naturalist 168, 62–75.

Yodzis, P., Innes, S., 1992. Body Size and Consumer-Resource Dynamics. The American Naturalist 139, 1151–1175.

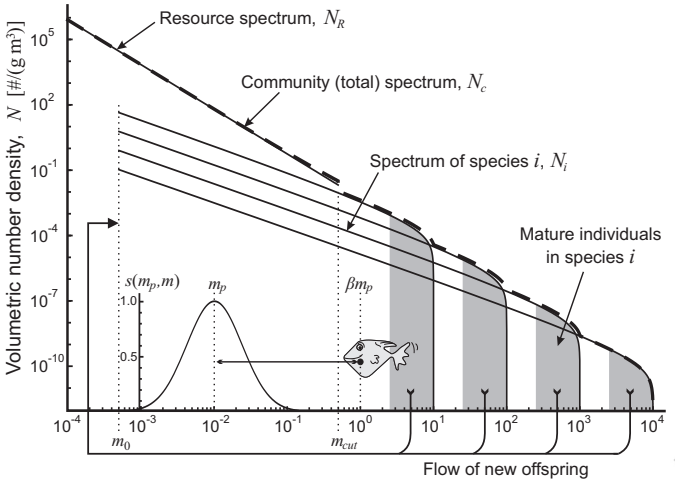

Figure 1: Illustration of the community model: resource spectrum (with cut-off m_{cut}) and four species size-spectra ($m_* = 2.5,\ 25,\ 250$, and 2 500 g) having off-spring of size m_0. Shaded regions mark the spawning stock from maturation size m_* to maximum asymptotic size M. The sum of all spectra gives the community spectrum. The spectra shown are the steady-state solutions from Andersen and Beyer (2006). Inset shows how individuals feed on smaller prey using a feeding kernel with a preferred PPMR of β.

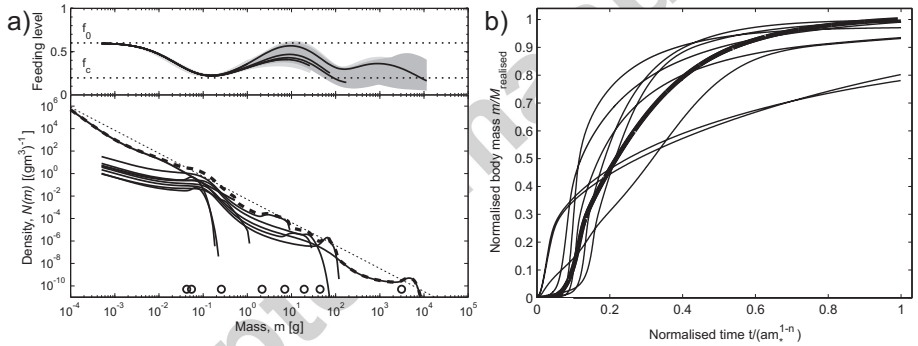

Figure 2: Example of an eight species cyclic state. a) Top: Feeding levels of the species along with the min/max (light grey) and the 25%/75% (dark grey) percentile values of the time-series. Dashed lines indicate initial f_0 and critical f_c feeding level. Bottom: The time-average of the resource and species spectra along with the community spectra (thick dashed). The idealised community spectrum $\kappa_c m^{-\lambda}$ (thin dashed) and the species maturation sizes m_* (circles). b) Time averaged growth curves for the species (thin lines) along with the biphasic growth curve (8) for a fixed feeding level that equals 75% of the time and size averaged feeding level experienced by the species (thick line). Growth curves are normalised with realised asymptotic size (y-axis) and generation time (x-axis) to enable comparison.

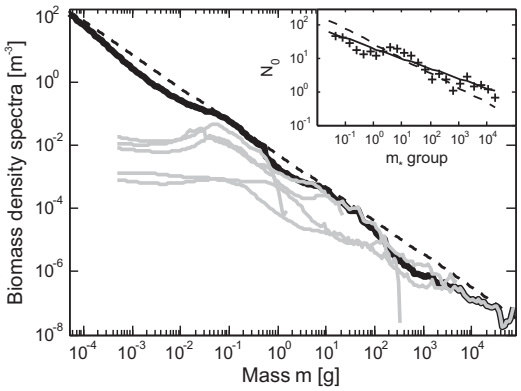

Figure 3: Mean species biomass spectra (grey lines) when species are divided into 5 logarithmic evenly distributed m_* groups. Also shown is the total mean community biomass spectrum (thick line), and the EQT community biomass spectrum $\kappa_c m^{1-\lambda}$ (dashed). Inset shows how offspring abundance (N_0) scales with m_* (data pooled in 25 log groups). Expected EQT scaling of N_0 is shown for $a = 0.86$ (dashed) and $a = 1$ (solid).

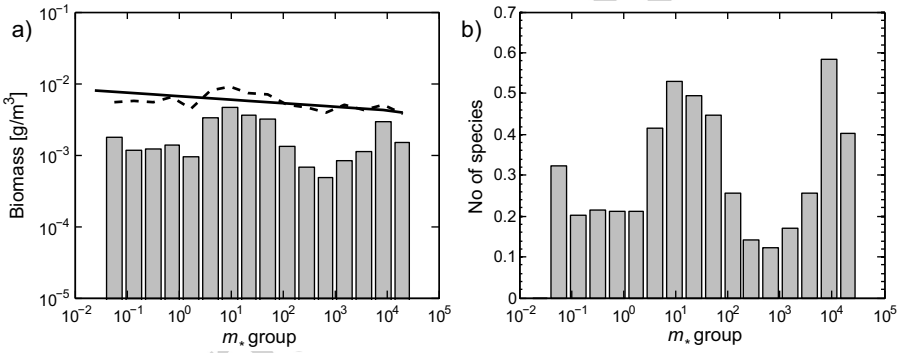

Figure 4: a) Distribution of biomass in different m_* groups. The expected distribution $B(m_*) \propto m_*^{n-q}$ is illustrated with the solid line. Dashed line shows biomass per species (bar values divided with bar values in b)). b) Mean no of species as a function of m_*. Species are pooled into 16 logarithmic groups.

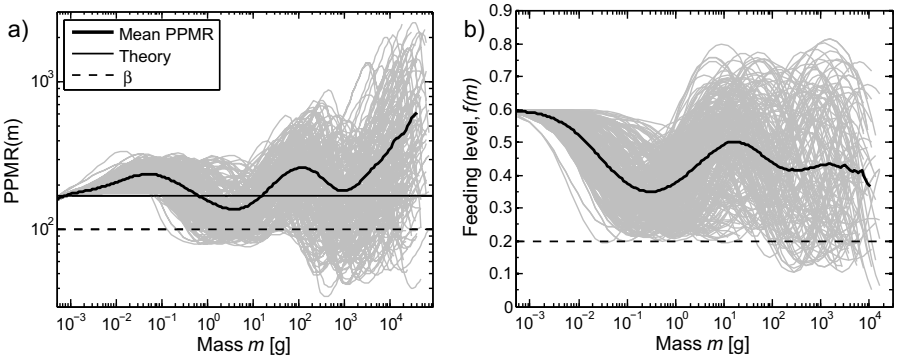

Figure 5: a) Realised PPMR from each food web (grey), mean realised PPMR across all simulations (thick black), realised PPMR prediction from equilibrium theory (thin black), and preferred PPMR β (thin dashed). b) Feeding level from each species (grey), and mean feeding level (thick black).

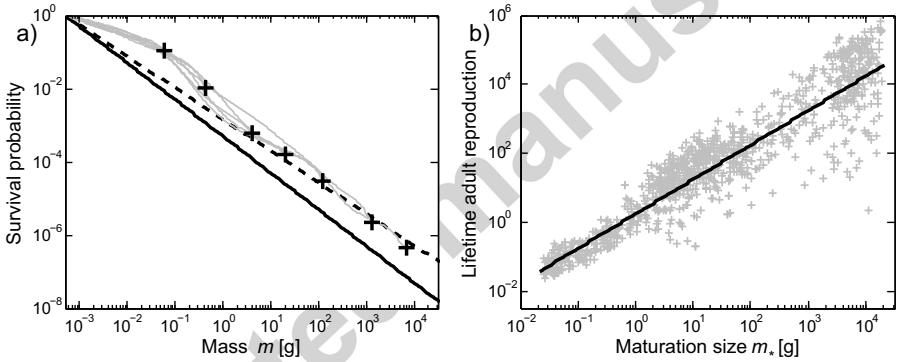

Figure 6: The components of the expected lifetime reproductive output. a) Probability of surviving to maturation size m_* (crosses) along with survival curves throughout life (grey line) for data pooled into 7 logarithmic groups. Expected $p \propto m_*^{-a}$ scaling from EQT is shown for $a = 0.86$ (dashed) and $a = 1$ (solid). b) Lifetime adult reproduction for all species (crosses) along with EQT $R_{\mathrm{adult}} \propto m_*$ expectation (line).

Table 1: Default parameter values for a temperature of 10°C (Appendix E).

Symbol	Value	Units	Parameter
Individual growth			
f_0	0.6	-	Initial feeding level
α	0.6	-	Assimilation efficiency
h	85	g^{1-n}/year	Maximum food intake
n	0.75	-	Exponent for max. food intake
k	10	g^{1-p}/year	Std. metabolism and activity
p	0.75	-	Exponent of std. metabolism
β	100	-	Preferred PPMR
σ	1	-	Width of feeding kernel
q	0.8	-	Exponent for search volume
Reproduction			
m_0	0.5	mg	Offspring mass
η_*	0.25	-	m_* rel. to asymptotic mass M
ϵ	0.1	-	Efficiency of offspring production
u	10	-	Width of maturation transition
Mortality			
ξ	0.1	-	Fraction of energy reserves
μ_0	0.84	g^{1-n}/year	Background mortality
Resource spectrum			
κ	$5 \cdot 10^{-3}$	$g^{\lambda-1}/m^3$	Magnitude of resource spectrum
λ	$2-n+q$	-	Slope of resource spectrum
r_0	4	g^{1-p}/year	Regeneration rate of resources
m_{cut}	0.5	g	Upper limit of resource spectrum

Appendix should be available as online material.

Appendix A. Derivation of predation mortality

Predators with a size between m and $m + dm$ have a food intake rate of $s(m_p, m)f(m)hm^n\theta N(m)dm$ for m_p sized prey. The total density of food available from all prey sizes to the predators in $[m\,; m + dm]$ is $\phi(m)$ (5), meaning that the mortality experienced by a m_p sized individual is:

$$\mu_{p,i}(m_p) = \sum_j \int \frac{s(m_p, m)f_j(m)hm^n\theta_{j,i}N_j(m)}{\phi_j(m)}\, dm. \tag{A.1}$$

The maximum food intake may be expressed as a function of $f(m)$, $v(m)$, and $\phi(m)$ via (6), such that the predation mortality can be written as:

$$\mu_{p,i}(m_p) = \sum_j \int s(m_p, m)(1 - f_j(m))v(m)\theta_{j,i}N_j(m)\, dm. \tag{A.2}$$

By using the EQT assumptions of constant feeding level and a power law community spectrum (cf. section 3) the mortality reduces to $\mu_p(m_p) = \overline{\theta}(1 - \overline{f}) \int s(m_p, m)v(m)\kappa_c m^{-\lambda}\, dm$, which can be solved analytically:

$$\mu_p(m_p) = \alpha_p m_p^{n-1}, \tag{A.3}$$

where $\alpha_p = \overline{\theta}(1 - \overline{f})\sqrt{2\pi}\kappa_c\gamma\sigma\beta^{1+q-\lambda} \exp\left[\frac{1}{2}\sigma^2(1 + q - \lambda)^2\right]$.

Appendix B. Available food and the physiological level of predation a

Using the EQT assumption of a power law community spectrum allows calculation of the available food density $\phi(m) = \overline{\theta} \int s(m_p, m)\kappa_c m_p^{-\lambda} m_p\, dm_p$:

$$\phi(m) = \alpha_\phi \overline{\theta}\kappa_c m^{2-\lambda}, \tag{B.1}$$

where $\alpha_\phi = \sqrt{2\pi}\sigma\beta^{\lambda-2} \exp\left[\frac{1}{2}\sigma^2(2 - \lambda)^2\right]$.

Using the EQT assumption of constant feeding level yielding $\lambda = 2 + q - n$ allows us to write $\overline{\theta}\kappa_c = \overline{f}h/(\alpha_\phi\gamma(1 - \overline{f}))$ by rearranging the expression of the feeding level (6). Using this and the definition of $\hbar$ allows writing $\alpha_p = c(\hbar + k)\beta^{2n-q-1}/\alpha$ where $c = \exp\left[\frac{1}{2}\sigma^2\left((1 + q - \lambda)^2 - (2 - \lambda)^2\right)\right] = 1.03 \approx 1$. Ultimately using the definition of f_c allows writing the physiological level of predation $a = \alpha_p/\hbar$ as:

$$a = c\frac{\overline{f}}{\overline{f} - f_c}\beta^{2n-q-1}/\alpha. \tag{B.2}$$

Appendix C. Calculating efficiency ϵ of offspring production

The efficiency of turning energy into offspring is denoted ϵ. It includes losses due to behavioural aspects, pre-hatching mortality, and that the energy contents in gonadic tissue is higher than in somatic tissue. It is a quantity that is difficult to measure, but for $n = p$ its value can be derived.

The energy (in units of mass) routed into reproduction (for $n = p$) is $\psi(m, m_*)\hbar m^n$ where $\hbar = \alpha\overline{f}h - k$. The energy of the produced offspring is then, $E_o(m) = \epsilon\psi(m, m_*)\hbar m^n$:

$$E_o(m) = \epsilon\hbar\eta_*^{1-n} m_*^{n-1} m. \tag{C.1}$$

From Gunderson (1997) we have the yearly mass-specific allocation to reproduction:

$$\varrho(m_*) = \varrho_0 \eta_*^{1-n} m_*^{n-1}, \tag{C.2}$$

where $\varrho_0 = 1.2\,\mathrm{g}^{1-n}/\mathrm{year}$ is obtained using least sum of squares in fitting the curve to the data for oviparous fish in Gunderson (1997). Equalling (C.2) and E_o/m allow us to determine the efficiency of offspring production ϵ:

$$\epsilon = \frac{\varrho_0}{\hbar} \approx 0.12. \tag{C.3}$$

Appendix D. Setting the search rate prefactor γ from initial feeding level f_0

Food for the smallest individuals in the spectra will be supplied by the background spectrum. If we assume that the resource spectrum is at carrying capacity κ then an equilibrium initial feeding level f_0 for the small individuals can be calculated using (6).

Alternatively we may specify an initial feeding level f_0 and derive one other parameter. By solving the feeding level for γ by using the analytical solution for the density of food $\phi(m)$ (B.1) we find γ as a function of f_0:

$$\gamma = \frac{f_0 h}{(1-f_0)\alpha_\phi \theta_{i,R} \kappa} \approx \frac{f_0 h \beta^{2-\lambda}}{(1-f_0)\sqrt{2\pi}\sigma\theta_{i,R}\kappa}. \tag{D.1}$$

Appendix E. Parameter estimation

Individual growth: From Kitchell and Stewart (1977) we obtain an estimate of specific dynamic action on 15 % of food consumption, and conservative estimates of egestion and excretion on 15 % and 10 % respectively. This results in an assimilation efficiency of $\alpha = 0.6$.

The maximum intake scales with a 0.6–0.8 exponent, with $n = 0.75$ being an approximate average value (Jobling, 1994). Andersen and Riis-Vestergaard (2004) provides a length-based relationship for the maximum intake rate based on a whiting study adopted for saithe. Using $m = 0.01l^3$ (m in g and l in cm) (Peters, 1983), and an energy content of 5.8 kJ/g (fish) or 4.2 kJ/g (invertebrates) (Boudreau and Dickie, 1992) yields a prefactor h for the maximal food intake on $83\,\mathrm{g}^{1-n}/\mathrm{year}$ or $114\,\mathrm{g}^{1-n}/\mathrm{year}$ (at 10°C). These intake values overestimate the intake of large individuals since Andersen and Riis-Vestergaard (2004) use an intake exponent of 0.67 instead of $n = 0.75$. Due to this a value of $h = 85\,\mathrm{g}^{1-n}/\mathrm{year}$ is selected, which also provides reasonable fits to 'cod-like' growth curves ($m_* = 5$ kg).

The standard metabolism scaling exponent p for fish is slightly higher than for other taxa, around 0.8 from intra- and interspecies measurements (Winberg, 1956; Killen et al., 2007). For simplicity we assume $p = n$. The first term (acquired energy) in the growth model (8) is $\alpha f(m) h m^n$ where the feeding level $f(m)$ is a decreasing function of body size (see *Results*). This has the effect that even when $n = p$ is assumed the acquired energy term still effectively scale with a smaller exponent than the maintenance term km^p in accordance with the experimental data on food intake and standard metabolism. Furthermore it is noted that this clearly makes the individuals in each functional species non-neutral. The bioenergetic consequences of $n \neq p$ has been explored in detail by Andersen et al. (2008).

The prefactor for standard metabolism can from Peters (1983) be determined to $6.5\,\mathrm{g}^{1-n}/\mathrm{year}$ if the diet is composed of only invertebrates and $4.7\,\mathrm{g}^{1-n}/\mathrm{year}$ if all the energy is from fish. Both values were corrected to 10°C using $Q_{10} = 1.83$ (Clarke and Johnston, 1999). It is assumed that energy costs due

to activity can be described with an activity multiplier on the standard metabolic rate. Estimations of activity costs are difficult to obtain, but activity multipliers are often reported in the range 1 to 3; e.g. 1.25 for North Sea cod (Hansson et al., 1996), 1.7 for dace (Trudel and Boisclair, 1996), and 1.44-3.27 for saithe (Andersen and Riis-Vestergaard, 2004) (however see also Rowan and Rasmussen (1996); He and Stewart (1997)). A reasonable value of the prefactor for the standard metabolism and activity costs is assumed to be $k = 10\,\mathrm{g}^{1-n}/\mathrm{year}$ corresponding to an activity multiplier in the range 1.5 to 2.1.

Food encounter: The preferred predator-prey mass ratio is set to $\beta = 100$ (Jennings et al., 2002) and the width of the selection function to $\sigma = 1$, which catches the general picture for at least cod and dab (Ursin, 1973). It should be noted that small organisms such as copepods have a larger σ of 3–4.5 (Ursin, 1974), but for simplicity and since focus is on species with rather large m_* the width σ will be held constant.

The exponent for swimming speed is $q = 0.8$ (Andersen and Beyer, 2006). The prefactor γ for the volumetric search rate is difficult to assess from the literature. An alternative approach is to determine it as a function of of initial feeding level f_0 via (D.1). Experience with the model shows that feeding level is a decreasing function of body size. This means that it is sensible to use an initial feeding level f_0 that is larger than the expected average feeding level $\overline{f}$. In this study a default value of $f_0 = 0.6$ is used. This along with default parameters yields $\gamma = 0.8 \cdot 10^4\,\mathrm{m}^3\mathrm{g}^{-q}/\mathrm{year}$ (Table 1). An alternative estimate of γ is possible by multiplying the prefactors for swimming speed (Ware, 1978) and swept reactive field area (reactive radius assumed equal to body length): $\gamma = 20.3 \cdot \pi \cdot 0.01^{-2/3}\mathrm{cm}^3\mathrm{g}^{-q}/\mathrm{s} \approx 4.3 \cdot 10^4\,\mathrm{m}^3\mathrm{g}^{-q}/\mathrm{year}$, which indeed justifies the use of $f_0 = 0.6$.

Mortality: Realistic energy reserve sizes may be $\xi \in [5\%;\ 20\%]$, and in the present study $\xi = 0.1$ is used. A widely used background mortality for 'cod-like' $m_* = 5\,\mathrm{kg}$ fishes is $\mu_b = 0.1\,\mathrm{year}^{-1}$, which yields $\mu_0 = 0.84\,\mathrm{g}^{1-n}/\mathrm{year}$.

Reproduction: The efficiency of offspring production was not found in the literature. However, an analytical expression may be obtained (for $n = p$) by combining the calculation of yearly mass-specific allocation to reproduction from the bioenergetic model (Appendix C) with empirical measurements (Gunderson, 1997), which yields $\epsilon = \varrho_0/\hbar \approx 0.1$. The fraction of asymptotic size to mature at is $\eta_* = 0.25$ (Andersen et al., 2008). Offspring mass is $m_0 = 0.5$ mg which corresponds to an egg diameter of 1 mm (Wootton, 1979; Chambers, 1997).

Resource spectrum: The carrying capacity of the resource spectrum should equal the magnitude of the community spectrum: $\kappa m^{-\lambda}$, with an exponent $\lambda = 2 - n + q = 2.05$ (Andersen and Beyer, 2006). The magnitude of the resource spectrum is set to $\kappa = 5 \cdot 10^{-3}\ \mathrm{g}^{\lambda-1}/\mathrm{m}^3$, which is comparable with findings from empirical studies (Rodriguez and Mullin, 1986). The constant for resource regeneration rate is $r_0 = 4\ \mathrm{g}^{1-p}/\mathrm{year}$ at $10^\circ\mathrm{C}$ (Savage et al., 2004). The cut-off of the resource spectrum is set to include mesoplankton, $m_{cut} = 0.5$ g.

Appendix F. Expected Lifetime Reproductive Success

The expected lifetime reproductive success can be split into two components: 1) the probability of surviving to become adult, and 2) lifetime reproduction per adult.

Appendix F.1. Survival probability

If we set $\frac{\partial N}{\partial t} = 0$ in (1) we may obtain the steady-state solution as:

$$N(m) = \frac{K(m_*)}{g(m, m_*)} \exp\left(-\int \frac{\mu(m)}{g(m, m_*)} dm\right), \tag{F.1}$$

where $K(m_*)$ is the constant from the integration along m. We notice that the probability of surviving from size m_0 to size m is $p_{m_0 \to m} = \exp\left(-\int_{m_0}^{m} \frac{\mu(m')}{g(m', m_*)} dm'\right)$, which along with $p_{m_0 \to m_0} = 1$ allow us to write the survival probability as:

$$p_{m_0 \to m} = \frac{N(m) g(m, m_*)}{N(m_0) g(m_0, m_*)}. \tag{F.2}$$

Appendix F.2. Lifetime adult reproduction

The amount of energy an adult belonging to a m_* population will spend on reproduction throughout its life is:

$$R_{life}(m_*) = \int_{t_*}^{\infty} p_{t_* \to t} \psi(m, m_*) E(m) dt,$$

where t_* is maturation age, and $\psi(m, m_*) E_i(m)$ the rate at which energy is allocated to reproduction. Noting that $g(m, m_*) = \frac{dm}{dt}$ allows us to write this as:

$$R_{life}(m_*) = \int_{m_*}^{M} p_{m_* \to m} \frac{\psi(m, m_*) E(m)}{g(m, m_*)} dm. \tag{F.3}$$

Appendix G. Details of Numerical Methods

The model is in the form of a series of coupled partial-integro-differential equations (1), one for each species with the size preference function (4) being the integral kernel. The equations are of the first order in mass (i.e. hyperbolic) in which case shocks could be formed in the solutions. However the integral kernel smooths out any discontinuities and the equations can be solved effectively and accurately using a standard semi-implicit upwind finite-difference scheme for solving PDEs (Press et al., 1992). The McKendrick-von Foerster PDE (1) is discretised by calculating $g(m, m_*)$ and $\mu(m)$ explicitly and making the time update implicit, to yield:

$$\frac{N_w^{i+1} - N_w^i}{\Delta t} + \frac{g_w^i N_w^{i+1} - g_{w-1}^i N_{w-1}^{i+1}}{\Delta m_w} = -\mu_w^i N_w^{i+1}, \tag{G.1}$$

where i denotes the time step, and w the grid index on the mass axis ($i, w \in \aleph^+$). First order approximations have been used for both the time and mass derivatives. The discretisation in mass is known as the upwind approximation since the derivative is calculated from w and $w-1$, which is possible since the growth function is non-negative. It is further noted that the ∂m approximation is semi-implicit since densities at time step $i+1$ are used. Equation (G.1) may be written as:

$$N_{w-1}^{i+1} \underbrace{\left(-\frac{\Delta t}{\Delta w_w} g_{w-1}^i\right)}_{A_w} + N_w^{i+1} \underbrace{\left(1 + \frac{\Delta t}{\Delta w_w} g_w^i + \Delta t \mu_w^i\right)}_{B_w} = \underbrace{N_w^i}_{C_w}, \tag{G.2}$$

which allows us to write an explicit solution for the density spectrum at the $i+1$ time step:

$$N_w^{i+1} = \frac{C_w - A_w N_{w-1}^{i+1}}{B_w}, \tag{G.3}$$

which can be solved iteratively since N_1^{i+1} is given by the boundary condition. The flux in the boundary $g(m_0, m_*) N(m_0, t)$ is equal to the reproduction flux of new recruits R (11) such that $g_0^i N_0^{i+1} = R$, which yields: $A_1 = 0$, and $C_1 = N_1^i + \frac{\Delta t}{\Delta m_1} R$.

This semi-implicit upwind scheme is very stable but diffusive. The third order QUICK (Quadratic Upwind Interpolation for Convective Kinematics) scheme along with the techniques by Zijlema (1996), which prevents overshooting problems introduced by the QUICK method, were used to check that numerical diffusion poses no problem for $\Delta t = 0.02$ years, and a m_w mass grid with 200 logarithmically evenly distributed points. To ensure stability the Courant condition (i.e. Press et al. (1992)):

$$\frac{|g_w^i|\Delta t}{\Delta m_w} \leq 1, \tag{G.4}$$

is prudent to fulfill. The essence of the criterion is that Δt should be small enough not to allow individuals to skip any mass cells m_w during their growth trajectory.

The grid m_w spans the offspring size m_0 to 85 kg to include maturation sizes up to the order of 20 kg. The grid for the background spectrum ends at m_{cut}, and the lower limit should be low enough to ensure food items for the smallest individuals in the functional species, i.e. 3 decades lower than m_0. Identical Δm_w is used for the background and species spectra to ease computations in the overlap $[m_0; m_{cut}]$.

To save computational time the ODEs for the background spectrum (15) are solved analytically. The solution at time $t_0 + \Delta t$ for the semi-chemostatic equation is:

$$N_R(m, t_0 + \Delta t) = K(m) - \Big(K(m) - N_R(m, t_0)\Big) e^{-[r_0 m^{p-1} + \mu_p(m)]\Delta t}, \tag{G.5}$$

where $K(m) = \frac{r_0 m^{p-1} \kappa m^{-\lambda}}{r_0 m^{p-1} + \mu_p(m)}$ is the effective carrying capacity at resource size m.

References

Andersen, K.H., Beyer, J.E., 2006. Asymptotic size determines species abundance in the marine size spectrum. The American Naturalist 168, 54–61.

Andersen, K.H., Beyer, J.E., Pedersen, M., Andersen, N.G., Gislason, H., 2008. Life-history constraints on the success of the many small eggs reproductive strategy. Theoretical Population Biology 73, 490–497.

Andersen, N.G., Riis-Vestergaard, J., 2004. Alternative model structures for bioenergetics budgets of a cruising predatory gadoid: incorporating estimates of food conversion and costs of locomotion. Can. J. Fish. Aquat. Sci. 61, 2413–2424.

Boudreau, P.R., Dickie, L.M., 1992. Biomass Spectra of Aquatic Ecosystems in Relation to Fisheries Yield. Can. J. Fish. Aquat. Sci. 49, 1528–1538.

Chambers, R.C., 1997. Environmental influences on egg and propagule sizes in marine fishes, in: Chambers, R.C., Trippel, E.A. (Eds.), Early Life History and Recruitment in Fish Populations. Chapman & Hall.

Clarke, A., Johnston, N.M., 1999. Scaling of metabolic rate with body mass and temperature in teleost fish. Journal of Animal Ecology 68, 893–905.

Gunderson, D.R., 1997. Trade-off between reproductive effort and adult survival in oviparous and viviparous fishes. Can. J. Fish. Aquat. Sci. 54, 990–998.

Hansson, S., Rudstam, L.G., Kitchell, J.F., Hildn, M., Johnson, B.L., Peppard, P.E., 1996. Predation rates by North Sea cod (Gadus morhua) – predictions from models on gastric evacuation and bioenergetics. ICES Journal of Marine Science 53, 107–114.

He, J., Stewart, D.J., 1997. Comment – Measuring the bioenergetic cost of fish activity in situ using a globally dispersed radiotracer (^{137}Cs). Can. J. Fish. Aquat. Sci. 54, 1953–1954.

Jennings, S., Warr, K.J., Mackinson, S., 2002. Use of size-based production and stable isotope analyses to predict trophic transfer efficiencies and predator-prey body mass ratios in food webs. MEPS 240, 11–20.

Jobling, M., 1994. Fish Bioenergetics. Fish and Fisheries Series 13, Chapman & Hall.

Killen, S.S., Costa, I., Brown, J.A., Gamperl, A.K., 2007. Little left in the tank: metabolic scaling in marine teleosts and its implications for aerobic scope. Proc. R. Soc. B 274, 431–438.

Kitchell, J.F., Stewart, D.J., 1977. Applications of a Bioenergetics Model to Yellow Perch (Perca flavescens) and Walleye (Stizostedion vitreum vitreum). J. Fish. Res. Board Can. 34, 1922–1935.

Peters, R.H., 1983. The ecological implications of body size. Cambridge University Press.

Press, W.H., Flannery, B.P., Teukolsky, S.A., Vetterling, W.T., 1992. Numerical Recipes in C : The Art of Scientific Computing. Cambridge University Press. Also available at: http://www.nr.com/.

Rodriguez, J., Mullin, M.M., 1986. Relation between biomass and body weight of plankton in a steady state oceanic ecosystem. Limnol. Oceanogr. 31, 361–370.

Rowan, D.J., Rasmussen, J.B., 1996. Measuring the bioenergetic cost of fish activity in situ using a globally dispersed radiotracer (^{137}Cs). Can. J. Fish. Aquat. Sci. 53, 734–745.

Savage, V.M., Gillooly, J.F., Brown, J.H., West, G.B., Charnov, E.L., 2004. Effects of Body Size and Temperature on Population Growth. The American Naturalist 163, 429–441.

Trudel, M., Boisclair, D., 1996. Estimation of fish activity costs using underwater video cameras. Journal of Fish Biology 48, 40–53.

Ursin, E., 1973. On the Prey Size Preferences of Cod and Dab. Meddelelser fra Danmarks Fiskeri- og Havundersgelser, N.S 7, 85–98.

Ursin, E., 1974. Search Rate and Food Size Preference in Two Copepods. ICES CM L/23, 1–13.

Ware, D.M., 1978. Bioenergetics of Pelagic Fish: Theoretical Change in Swimming Speed and Ration with Body Size. J. Fish. Res. Board. Can. 35, 220–228.

Winberg, G.G., 1956. Rate of metabolism and food requirements of fishes. Fish. Res. Board Can. Translation Series No. 194, 1–253.

Wootton, R.J., 1979. Energy Costs of Egg Production and Environmental Determinants of Fecundity in Teleost Fishes. Symp. zool. Soc. Lond. 44, 133–159.

Zijlema, M., 1996. On the construction of a third-order accurate monotone convection scheme with application to turbulent flows in general domains. International Journal for Numerical Methods in Fluids 22, 619–641.